Journal of Marine Science and Technology, Vol. 27, No. 1, pp. 28-34 (2019)
DOI: 10.6119/JMST.201902_27(1).0004

# APPLICATION OF RANDOM GEOMETRIC IMPERFECTION METHOD TO NONLINEAR BUCKLING ANALYSIS OF SPHERICAL SHELL

Zhixin Xiong[1, 3], Zhiquan Huang[2], Xiaochuan Yu[3], and Jiamin Guo[1]

Key words: spherical shell, random geometric imperfection, buckling load, ABAQUS.

## ABSTRACT

This paper focuses on spherical shells with random geometric imperfections under uniform external pressure. An extensive numerical investigation is performed to calculate the buckling loads of perfect and imperfect spherical shells. To discuss the effects of initial geometric imperfections, a finite element analysis model of the perfect spherical shell is considered to obtain its first 60 modes. Then, the consistent imperfect buckling analysis method is applied to analyze the nonlinear stability of the spherical shells with geometric imperfections. The shapes of the shell in the 1st to 20th eigenmode are considered. A lower buckling load is found corresponding to the 17th eigenmode, which is different from the analysis-derived opinion that the buckling stress is often observed in the 1st eigenmode. Moreover, the random geometric imperfection method is applied to imperfect spherical shells by incorporating random geometric imperfections. The statistical analysis of numerical results from 200 random cases indicates that the calculated ultimate strength can be lowered to 5.58 MPa in this example, which is approximately 87% of the result from the 1st eigenmode. Therefore, it may be concluded that the random geometric imperfection method can be used for analyzing the stability of structures with imperfections to obtain realistic results.

## I. INTRODUCTION

The spherical configuration is usually considered ideal for deep submersibles. However, various imperfections exist in structures or their materials. Such initial geometric imperfections may greatly influence the load-carrying capacity of spherical pressure hulls. Many experiments have demonstrated that the experimental buckling loads of spherical shells are lower than the corresponding theoretical capacities (Pan and Cui, 2010).

Since the 1960s, a few researchers have focused on investigating how the imperfections of spherical shells affect the loading capacities of various structures. Krenzke and Kiernan (1965) conducted four series of tests on more than 200 small spherical models with different imperfections and derived an empirical formula. Even in the case of machined perfect spherical shells, the actual buckling loads were found to be only 70% of the ideal values. Hutchinson (1967) investigated the initial postbuckling behavior of a spherical shell under external pressure based on Koiter's general theory. The effects of imperfections on the buckling strength of structures were also examined. Koga and Hoff (1969) studied the buckling and postbuckling behaviors of complete spherical shells under the assumption that random imperfections and the resulting elastic deformations are symmetric along a few diameters of the shell. Kao proposed a formula based on Donnell-type nonlinear cylindrical shell theory to describe strain-displacement relationships by considering initial imperfections (Kao, 1972).

Morton et al. (1981) interpreted experimental results in the light of numerical analysis, imperfection sensitivity, and design codes. Galletly et al. (1987) used a buckling program to calculate plastic buckling/collapse pressures of externally pressurized imperfect hemispherical shells. Fan (1989) investigated the postbuckling behavior and imperfection sensitivity of spherical shells with amplitude modulation. The buckling modes were assumed to be the form of Legendre polynomials with an exponential function as a modulating factor. Two axisymmetric initial imperfection shapes were studied, namely, localized increased-radius type and Legendre polynomial. Galletly and Blachut (1991) showed that the test results of 28 welded hemispherical shells obtained at the David Taylor Model Basin (DTMB) can be predicted quite well by using simplified shape imperfections. Moreover, they pointed out that the residual stress was not considered, and this might decrease a spherical shell's buckling resistance to external pressure. Blachut and Galletly (1995) discussed seven 580-mm-diameter spun steel hemispherical shells

*Paper submitted 07/11/18; revised 10/29/18; accepted 01/07/19. Author for correspondence: Xiaochuan Yu (e-mail: xyu5@uno.edu).*

[1] *College of Ocean Science and Engineering, Shanghai Maritime University, Shanghai 201306, China.*
[2] *College of Logistic Engineering, Shanghai Maritime University, Shanghai 201306, China.*
[3] *School of Naval Architecture and Marine Engineering, University of New Orleans, New Orleans, LA 70148, USA.*

subjected to external pressure. They reported that the techniques employed proved to be entirely reliable for predicting the collapse strength of the spun steel hemispheres.

Since 2000, researchers from developing countries, for example, China, have published a series of papers on the buckling loads of deep-sea submersibles. Pan and Cui (2010) further modified the formula and pointed out that thin shells are more sensitive to imperfections than thick shells. Yu et al. (2017) comprehensively analyzed the effects of specific imperfections caused by welding on the strength of shells by studying residual stress and deformations.

In addition, consideration of random defects in a shell is important. In the early stage, researchers have focused on formulating probability functions by using measured data (Elishakoff and Arbocz, 1982; Ivanova and Trendafilova, 1992; Arbocz and Hol, 1995; Chryssanthopoulos and Poggi, 1995). With the development of computer technology, the Monte Carlo simulation method has been used extensively to study random defects in shells. Bielewicz and GórskI (2002) used random variables or random fields to describe geometric imperfections in shells. Subsequently, they employed the Monte Carlo method combined with a finite element analysis (FEA) program. Schenk and Schuëller (2003) modeled geometric imperfections as a two-dimensional Gaussian stochastic process with prescribed second-moment characteristics based on a data bank of measured imperfections. In 2007, they numerically generated the realizations of both boundary and geometric imperfections based on the Karhunen-Loève expansion (Schenk and Schuëller, 2007). Papadopoulos and Papadrakakis (2005) described initial geometric imperfections as a two-dimensional univariate stochastic field with statistical properties. In the stochastic vulnerability-based robust design procedure of isotropic shell structures, uncertain initial geometric as well as material and thickness properties are modeled as a random field (Papadopoulos and Lagaros, 2009). To investigate the direct global buckling mode of thick-walled tubes, Fyllingen et al. (2007) modeled the geometric imperfections by assuming Gaussian random fields. Caitríonade et al. (2012) characterized the variation in radius as a two-dimensional random field and developed an algorithm to generate realizations of this field. However, the random geometric imperfection method has seldom been applied for calculating the limit strength of spherical shells. In fact, almost all spherical shells have initial geometric imperfections that originate during manufacture.

In this study, random geometric imperfections of pressurized spherical shells were considered in a FEA model, and a probabilistic method was applied. The spherical shells were assumed to be made of titanium alloy. Commercial FEA software ABAQUS was employed for performing the FEA.

## II. LINEAR BUCKLING ANALYSIS OF SPHERICAL HULL

Usually, buckling loads from the 1st eigenmode method are applied in engineering projects for design purpose. However, these loads do not naturally represent the worst case. It may be more important to perform nonlinear buckling analysis based on a higher-order mode method. For example, Zhang et al. (2018) presented 360 types of geometrically and materially nonlinear analysis, all of which are based on the 1st buckling-mode (eigenmode) imperfection for geometrically imperfect spherical pressure hulls.

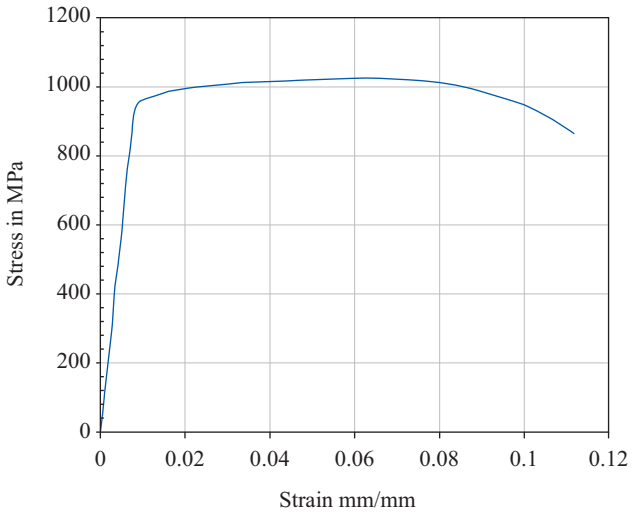


**Fig. 1. Stress-strain curve of titanium alloy (Pranesh et al., 2017).**

In this study, we calculated buckling loads up to the 60th-order eigenmode.

### 1. Geometric Parameters and Material Properties

Herein, a manned vehicle is considered and discussed. Its spherical pressure shell was made of titanium alloy. Its elastic modulus $E$ was 114,800 MPa, Poisson ratio $\upsilon$ was 0.3, and yield strength $\sigma_S$ was 828 MPa. The stress-strain curve is shown in Fig. 1 (Pranesh et al., 2017). The minimum internal diameter was 2,100 mm, and the uniform wall thickness $t$ was 10 mm.

### 2. Linear Buckling Analysis

Linear buckling analysis was performed to obtain the elastic critical buckling loads of the perfect structure. In ABAQUS, the elastic critical buckling behavior can be determined as follows:

$$\left(\lambda_i K\right)\overline{\upsilon_i} = 0 \tag{1}$$

where $\lambda_i$ are eigenvalues (elastic critical buckling resistance), $K$ is the tangent stiffness matrix, and $\overline{\upsilon_i}$ are buckling mode shapes (eigenvectors).

The obtained buckling mode shapes did not represent the actual magnitudes of deformation at the critical buckling loads because they have been normalized.

*1) Buckling Loads of Spherical Shells*

For perfect spherical shells, the critical elastic buckling load of a complete sphere under external pressure can be calculated

**Table 1. Linear buckling loads of a perfect spherical shell determined using a theoretical formula and the FEA method.**

| T (mm) | Rm (mm) | Calculated results of elastic buckling | | | |
|---|---|---|---|---|---|
| | | ①Theory results | ②This paper | (Pranesh et al., 2017) | ②and①Relative error (%) |
| 5 | 1052.5 | 3.14 | 3.14 | 3.12 | 0.00 |
| 6 | 1053 | 4.51 | 4.51 | -- | 0.02 |
| 7 | 1053.5 | 6.14 | 6.13 | -- | 0.16 |
| 8 | 1054 | 8.01 | 8.01 | -- | 0.00 |
| 9 | 1054.5 | 10.12 | 10.12 | -- | 0.00 |
| 10 | 1055 | 12.49 | 12.48 | 12.41 | 0.08 |
| 11 | 1055.5 | 15.09 | 15.09 | -- | 0.00 |
| 12 | 1056 | 17.94 | 17.95 | -- | 0.06 |
| 13 | 1056.5 | 21.04 | 21.02 | -- | 0.08 |
| 14 | 1057 | 24.38 | 24.37 | -- | 0.04 |
| 15 | 1057.5 | 27.96 | 27.94 | 27.69 | 0.07 |

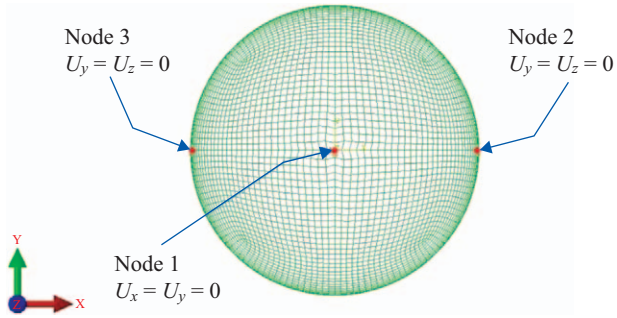


**Fig. 2. Boundary conditions of FE model.**

analytically as follows:

$$p_{cr} = \frac{2E}{\sqrt{3(1-\mu^2)}}\left(\frac{t}{R_m}\right)^2 \quad (2)$$

where $p_{cr}$ is the critical elastic buckling stress, $E$ is the Young's modulus of the material, $t$ is the thickness of the sphere, and $R_m$ is the mean radius of the sphere.

In ABAQUS, the shell element is adopted in the FEA model. In total, the model comprises 23,330 nodes and 7,776 elements. The boundary conditions employed in the FEA model are shown in Fig. 2. For node 1, the displacements along the $x$- and $y$-directions are restrained. For nodes 2 and 3, the displacements along the $y$- and $z$-directions are restrained, that is, $U_x = U_y = 0$. In this way, the boundary conditions can help hold rigid body movements without affecting relative deformation considerably.

We considered a thin spherical shell with internal diameter 2,100 mm as an example. Its linear buckling load was calculated using a theoretical formula and the FEA method. The corresponding results are summarized in Table 1.

From Table 1, the numerical results are very close to the theoretical values. For all cases, the maximal relative error was less than 0.2%.

**Table 2. Buckling mode shapes of first 10 modes.**

| The nth mode | 1th | 2nd | 3rd | 4th |
|---|---|---|---|---|
| Graphic mode shape | 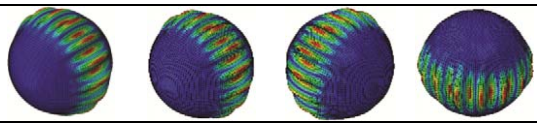 | | | |
| The nth mode | 5th | 6th | 7th | 8th |
| Graphic mode shape | 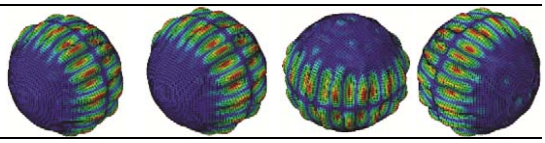 | | | |
| The nth mode | 9th | 10th | | |
| Graphic mode shape | 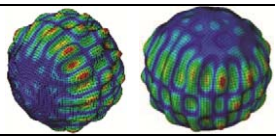 | | | |

*2) Buckling Shapes and Related Buckling Loads*

The first 60 mode shapes were easily obtained by using ABAQUS. Because of the symmetric properties of both the shell structure and external water pressure, a few modes appeared in pairs. The first 10 mode shapes are graphically shown in Table 2, where the scale ratio is 1:100.

Among the different modes from the 1st mode to the 60th mode, the critical buckling load increased from 12.479 to 12.525 MPa, which is an increase of 0.4%. This result is consistent with previous findings (Teng and Rotter, 2004).

## III. NONLINEAR BUCKLING ANALYSIS OF SPHERICAL SHELLS BASED ON THE CONSISTENT IMPERFECT METHOD

The maximum loading capacity of this shell under the per-

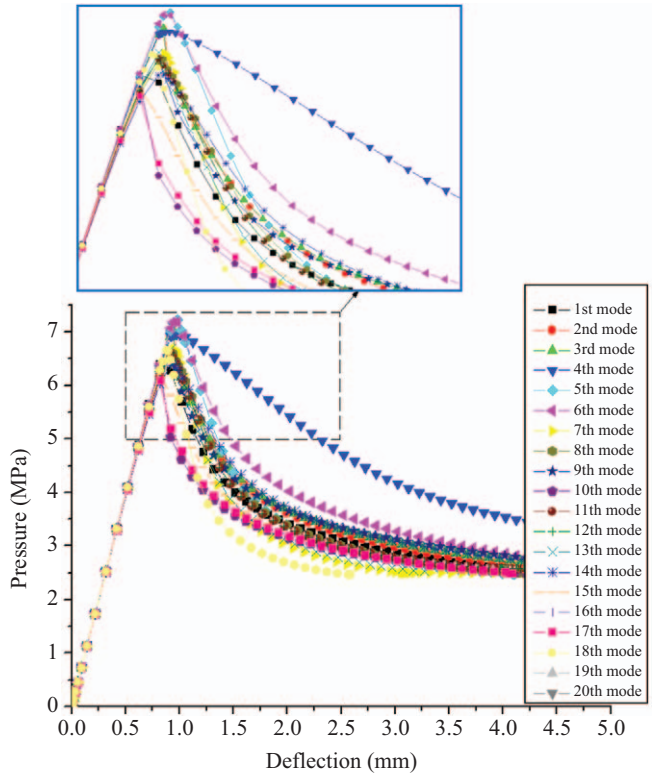


**Fig. 3. Pressure vs. deflection of spherical shells (with initial deflection of 1.7583 mm).**

fect condition was 12.51 MPa (Pranesh et al., 2017). We used the Riks method as the nonlinear solver to estimate nonlinear buckling loads. In the calculation, geometric nonlinearities were considered as large deformations in ABAQUS. In addition, the material was assumed to be plastic, as indicated in Fig. 1. First, the first 20 mode shapes obtained through linear buckling analysis were used directly in the consistent imperfect mode method as the initial mode shapes. To compare the results with those obtained using the random defect method, the maximum magnitude of imperfection was set to 1.7583 mm, which is the same as the value derived in Section IV(2). This ensures that the comparison between both methods is more meaningful. The initial displacements at each node for a certain mode can be scaled proportionally. Those displacements are considered initial geometric imperfections in nonlinear analysis.

Fig. 3 shows the relationship between pressure increase and deflection. From the magnified part shown in Fig. 3, it can be concluded that the 17$^{th}$ mode corresponds to the worst case, that is, the minimum buckling load is 6.11 MPa. As indicated in Fig. 3, the maximum elastic-plastic buckling load occurred for most modes when the deflection was approximately 1.0 mm. At deflections greater than 1.0 mm, the buckling load may decrease significantly with increasing deflection.

For each mode, the maximum loading capacity values are listed in Table 3.

As indicated in Fig. 3 and Table 3, it can be concluded that the structure is sensitive to the initial geometric imperfections.

**Table 3. Maximum loading capacity under initial geometry imperfections based on eigenvalue buckling modes.**

| Mode | 1 | 2 | 3 | 4 | 5 |
|---|---|---|---|---|---|
| Maximum loading capacity (MPa) | 6.39 | 7.01 | 7.02 | 6.96 | 7.23 |
| Mode | 6 | 7 | 8 | 9 | 10 |
| Maximum loading capacity (MPa) | 7.19 | 6.68 | 6.60 | 6.60 | 6.31 |
| Mode | 11 | 12 | 13 | 14 | 15 |
| Maximum loading capacity (MPa) | 6.61 | 6.61 | 6.68 | 6.38 | 6.20 |
| Mode | 16 | 17 | 18 | 19 | 20 |
| Maximum loading capacity (MPa) | 6.12 | 6.11 | 6.66 | 6.18 | 6.18 |

Moreover, the 1$^{st}$ buckling mode may not correspond to the worst initial case. To determine the worst initial imperfection, it is necessary to tentatively consider the first several modes as the initial imperfection.

## IV. NONLINEAR BUCKLING ANALYSIS OF SPHERICAL HULL WITH RANDOM GEOMETRIC IMPERFECTIONS

### 1. Normal Distribution of Geometric Imperfection

In real engineering design, the random imperfection method should be more applicable and reliable. The imperfections of spherical shells can be assumed to follow a normal distribution (Pranesh et al., 2017). Imperfections may be caused by different processes such as fabrication and welding.

For an imperfect model, the relationship between the actual and theoretical coordinates of each node can be written as follows:

$$\left|X_i - X_{i0}\right| \le R \tag{3}$$

where $X_i$ is the 3D coordinate of node $i$ in a real model; $X_{i0}$ is the 3D coordinate of node $i$ in an ideally perfect model; and $R$ is the maximum geometric imperfection at each node of the structure.

The initial deflection at each node is a variable defined as $x = X_i - X_{i0}$. It can be assumed to follow a normal distribution:

$$f(x) = \frac{1}{\sqrt{2\pi}\sigma} e^{\frac{(x-\mu)^2}{2\sigma^2}} \tag{4}$$

where $f(x)$ is the probability density function, $\mu$ is the expected value, and $\sigma$ is the standard deviation.Therefore, the probability distribution of 3D coordinates at each node $i$ in the real model can be expressed as follows:

$$\begin{aligned} &P\left\{X_{i0} - R < X_i \le X_{i0} + R\right\} \\ &= P\left\{\frac{X_{i0} - R - X_{i0}}{\sigma} < \frac{X_i - X_{i0}}{\sigma} \le \frac{X_{i0} + R - X_{i0}}{\sigma}\right\} \end{aligned} \tag{5}$$

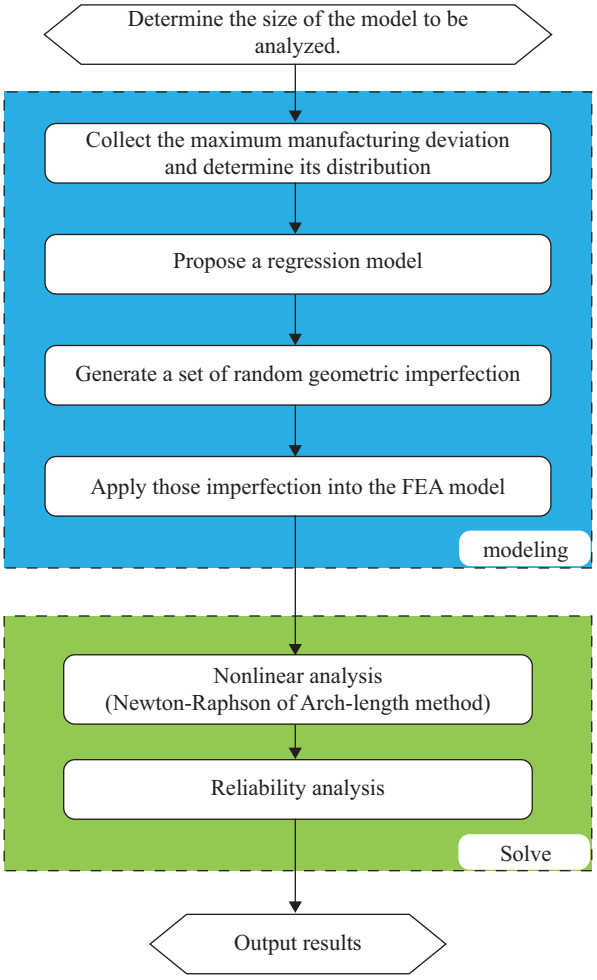


**Fig. 4. Flowchart of the random geometric imperfection method.**

where $P(x)$ is the accumulated probability.

Based on (Elishakoff, 1999), the probability of the node coordinates within the error range was 99.73% when the ratio between the maximum geometric imperfection and its standard deviation was 3.0 (that is, $R/\sigma = 3$). This is also called the "Three Sigma rule." Furthermore, the aforementioned equations can be transformed as follows:

$$\sigma = R / n \tag{6}$$

where $n$ is a value between 2 and 6.

The flowchart for calculating the maximum loading capacity of a spherical shell under pressure by using the random deflection method is shown in Fig. 4.

## 2. FEA Model of a Spherical Shell with Random Geometric Imperfections

In the following sections, the random geometric imperfection method is used to analyze the stability of spherical shells under pressure. The maximum allowable geometric imperfection is approximately 0.5% of the nominal mean radius (DNV, 2009).

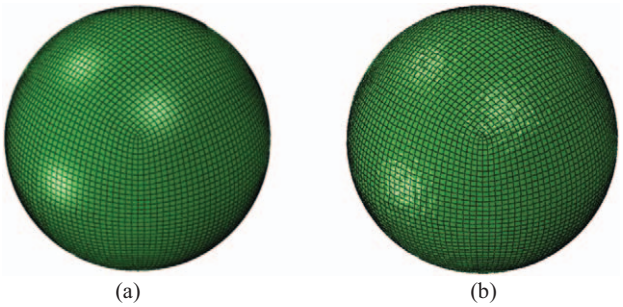


**Fig. 5. (a) Mesh of a perfect spherical shell. (b) Mesh of a spherical shell with random imperfections.**

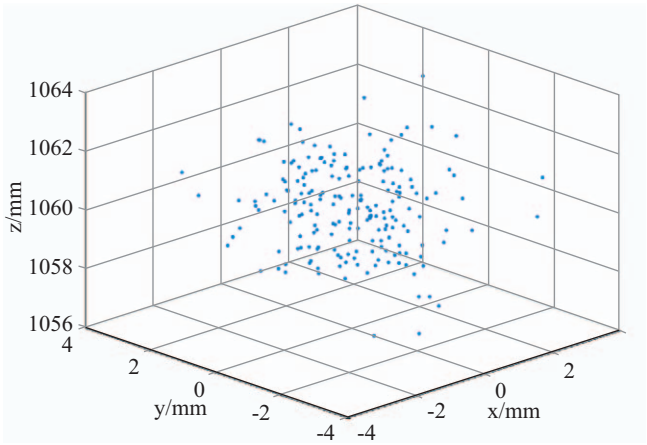


**Fig. 6(a). Distribution of 200 random imperfections at this node.**

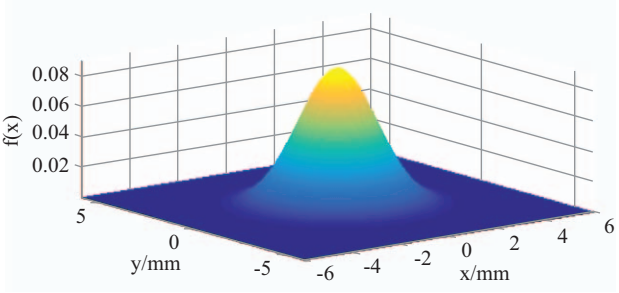


**Fig. 6(b). Probability density function of random geometric imperfections.**

For this sphere, the maximum allowable geometric imperfection $R$ was approximately 5.275 mm. According to the "Three Sigma rule" (Elishakoff, 1999), the standard deviation of geometrical imperfections σ was 5.275/3 = 1.7583 mm if $n$ is set to 3.

Fig. 5(a) represents a perfect shell, and Fig. 5(b) represents an imperfect shell with random geometric imperfections.

The distribution of random geometric imperfections at a certain node, as shown in Fig. 5(b), can be visualized in Fig. 6(a), with its median value at 0, 0, and 1060 mm. Furthermore, Fig. 6(b) presents the normal distribution of these geometric imperfections.

**Table 4. Maximum loading capacity under random initial geometry imperfections.**

| Maximum loading capacity (MPa) | | | | |
|---|---|---|---|---|
| 7.08 | 7.54 | 7.61 | 7.34 | 7.48 |
| 7.07 | 7.10 | 7.29 | 7.43 | 7.28 |
| 7.52 | 7.68 | 6.92 | 7.38 | 7.27 |
| 6.96 | 7.61 | 7.51 | 7.55 | 7.11 |
| 7.56 | 6.49 | 7.28 | 7.25 | 7.10 |
| 7.57 | 7.37 | 7.24 | 7.35 | 6.84 |
| 7.23 | 7.45 | 7.28 | 7.29 | 7.27 |
| 7.65 | 7.69 | 7.83 | 6.84 | 6.89 |
| 6.93 | 7.28 | 7.67 | 7.66 | 7.43 |
| 6.91 | 7.56 | 7.25 | 7.24 | 7.25 |
| 7.29 | 7.34 | 7.21 | 7.30 | 7.40 |
| 7.28 | 6.83 | 7.38 | 7.24 | 7.59 |
| 7.13 | 7.47 | 7.49 | 7.55 | 7.52 |
| 7.39 | 7.51 | 6.94 | 7.79 | 6.82 |
| 7.35 | 6.33 | 7.43 | 6.89 | 7.33 |
| 7.27 | 6.31 | 7.04 | 7.26 | 6.57 |
| 7.45 | 6.50 | 7.02 | 7.16 | 7.02 |
| 7.41 | 7.44 | 6.97 | 7.44 | 6.98 |
| 7.20 | 6.74 | 6.30 | 7.44 | 7.67 |
| 7.03 | 7.23 | 7.37 | 7.35 | 7.22 |
| 7.08 | 7.61 | 7.70 | 7.24 | 7.18 |
| 6.97 | 7.23 | 7.70 | 6.91 | 7.50 |
| 7.11 | 7.49 | 6.85 | 6.93 | 7.58 |
| 7.33 | 7.25 | 7.53 | 7.00 | 7.40 |
| 7.24 | 7.37 | 7.49 | 7.18 | 7.54 |
| 7.29 | 7.13 | 7.34 | 7.23 | 7.52 |
| 7.57 | 7.43 | 7.36 | 7.31 | 7.09 |
| 7.25 | 7.23 | 7.70 | 7.41 | 7.24 |
| 7.73 | 7.00 | 7.13 | 6.82 | 6.32 |
| 7.29 | 7.28 | 7.73 | 6.93 | 6.91 |
| 7.10 | 7.24 | 7.32 | 7.09 | 7.54 |
| 7.33 | 6.94 | 7.46 | 7.26 | 7.46 |
| 7.14 | 7.27 | 7.10 | 7.40 | 7.50 |
| 7.41 | 7.03 | 7.19 | 7.42 | 7.19 |
| 6.80 | 6.83 | 6.91 | 6.80 | 7.11 |
| 6.97 | 6.31 | 7.14 | 7.25 | 7.19 |
| 7.41 | 6.99 | 7.39 | 7.19 | 7.46 |
| 7.47 | 6.41 | 7.11 | 7.40 | 6.75 |
| 5.58 | 7.53 | 7.25 | 6.99 | 7.41 |
| 7.39 | 6.88 | 7.40 | 7.26 | 7.17 |

## 3. Results and Discussions

Two hundred initial geometric imperfections can be generated using MATLAB. The maximum loading capacity values obtained in 200 simulations are summarized in Table 4, with the minimum, maximum, and mean values being 5.58 MPa, 7.83 MPa, and 7.23 MPa, respectively. If compared with the result of 12.51 MPa calculated using the perfect model (Pranesh et al., 2017), they are approximately 45.9%, 64.4%, and 59.5%, respectively. The results show that the maximum loading capacity of the spherical shell structure is very sensitive to the initial geometric imperfection, as is consistent with the findings of previous studies (Pan and Cui, 2010; Pranesh et al., 2017).

**Table 5. Probability confidence level corresponding to each critical stress.**

| Mode | Maximum | Probability of |
|---|---|---|
| 1 | 6.39 | 99.57 |
| 2 | 7.01 | 75.41 |
| 3 | 7.02 | 74.42 |
| 4 | 6.96 | 80.06 |
| 5 | 7.23 | 50.00 |
| 6 | 7.19 | 54.97 |
| 7 | 6.68 | 95.72 |
| 8 | 6.60 | 97.55 |
| 9 | 6.60 | 97.55 |
| 10 | 6.31 | 99.80 |
| 11 | 6.61 | 97.37 |
| 12 | 6.61 | 97.37 |
| 13 | 6.68 | 95.72 |
| 14 | 6.38 | 99.60 |
| 15 | 6.20 | 99.94 |
| 16 | 6.12 | 99.97 |
| 17 | 6.11 | 99.98 |
| 18 | 6.66 | 96.26 |
| 19 | 6.18 | 99.95 |
| 20 | 6.18 | 99.95 |

Based on the "Three Sigma rule," the design critical load is as follows:

$$\sigma_\sigma = \mu - 3\sigma = 6.27 \text{ MPa} \tag{7}$$

Its probability reliability is 99.87%.

After we obtained the results using the random geometric imperfection method, the results obtained using the consistent imperfection mode method can be re-evaluated on the basis of reliability analysis. The calculated probability is summarized in Table 5.

In addition, the maximum allowable pressure derived using the local dimple method is 7.05 MPa (Pan and Cui, 2010), and its reliability is approximately 71.29%.

It can be deduced from Table 5 that the lower-order buckling mode need not represent the worst mode initial geometric imperfection. For example, with the consistent imperfection mode, the 5$^{th}$ mode can produce the maximum loading capacity of 7.23 MPa, with the corresponding reliability of only 50%. If this value is selected as the design value, it would certainly lead to a risk.

## V. CONCLUSIONS

Based on the aforementioned results and discussions, it can be concluded that the stability of pressurized spherical shells is

sensitive to initial geometric imperfections, which is consistent with previous findings (Pan and Cui, 2010).

In this study, the maximum initial geometric imperfection of 0.5% of the nominal mean radius was incorporated into FEA models. First, the consistent imperfection mode method was applied to calculate the maximum loading capacity. The 1st-order buckling mode of the structure did not guarantee the minimum buckling strength. Instead, the results from the 17th-order mode yielded the minimum value of 6.11 MPa, lower than the value obtained from the traditional 1st-order mode model. This indicates that the stability of a spherical shell under pressure with the lowest-order buckling mode of the structure as the initial geometric imperfection distribution mode is not necessarily the most unfavorable value.

In addition, the random geometric imperfection method can be applied. A normal distribution function was utilized to represent the random distribution of imperfections in reality. In total, 200 simulations were completed to ensure a more accurate and reliable maximum loading capacity physically. The calculations showed that the minimum value stood at approximately 87% of the result obtained using the 1st eigenmode method and approximately 79% of the result obtained using the local dimple method. Overall, the calculated maximum loading capacity of the spherical shell was approximately 45% of the perfect structural limit strength for this example.

Finally, the imperfections caused by welding were not considered in this study. However, such imperfections do exist invariably in the manufacture of spherical shells for deep-sea submersible vehicles. This will be considered in our future work.

## ACKNOWLEDGEMENTS

This work was supported by two grants. One is the National Science Foundation, China (Grant Number: 51609134), and the other is the State Key Laboratory of Ocean Engineering at Shanghai Jiao Tong University (Grant Number: 1610).

## REFERENCES

Arbocz, J. and J. M. A. M. Hol (1995). Collapse of axially compressed cylindrical shells with random imperfections. Thin-Walled Structures 23(1-4), 131-158.

Bielewicz, E and J. Górski (2002). Shells with random geometric imperfections simulation—based approach. International Journal of Non-Linear Mechanics 37, 777-784.

Blachut, J. and G. D. Galletly (1995). Buckling strength of imperfect steel hemispheres. Thin-Walled Structures 23, 1-20.

Caitríonade P., K. Cronin, J. P. Gleeson and D. Kelliher (2012). Statistical characterisation and modelling of random geometric imperfections in cylindrical shells. Thin-Walled Structures 58, 9-17.

Chryssanthopoulos, M. K. and C. Poggi (1995). Stochastic imperfection modelling in shell buckling studies. Thin-Walled Structures 23(1-4), 179-200.

Det Norske Veritas. (2009). Rules for Classification and Construction. I Ship Technology-5 Underwater Technology-2 Manned Submersibles. Norway: DNV-GL, 136.

Elishakoff, I. and J. Arbocz (1982). Reliability of axially compressed cylindrical shells with random axisymmetric imperfections. International Journal of Solids and Structures 18(7), 563-585.

Elishakoff, I. (1999). Probabilistic Theory of Structures. 2nd ed. Dover Publications, New York, USA, 78-83.

Fan, Q. S. (1989). Post-buckling behavior and imperfection sensitivity of spherical shells based on nonlinear elastic stability theory. Thin-Walled Structures 8(1), 1-18.

Fyllingen, Ø., O. S. Hopperstad and M. Langseth (2007). Stochastic simulations of square aluminum tubes subjected to axial loading. International Journal of Impact Engineering 34, 1619-1636.

Galletly, G. D., J. Blachut and J. Kruzelecki (1987). Plastic buckling of imperfect hemispherical shells subjected to external pressure. Proceedings of the Institution of Mechanical Engineers, Part C: Journal of Mechanical Engineering Science 201(3), 153-170.

Galletly, G. D. and J. Blachut (1991). Buckling design of imperfect welded hemispherical shells subjected to external pressure. Proceedings of the Institution of Mechanical Engineers, Part C: Journal of Mechanical Engineering Science 205(3), 175-188.

Hutchinson, J. W. (1967). Imperfection sensitivity of externally pressurized spherical shells. Journal of Applied Mechanics 4, 49-55.

Ivanova, J. and Trendafilova I. (1992). A stochastic approach to the problem of stability of a spherical shell with initial imperfections. Probabilistic Engineering Mechanics 7(4), 227-33.

Kao, R. (1972). Note on buckling of spherical caps with initial asymmetric imperfections. Journal of Applied Mechanics, Transactions of the ASME, Series E39(3), 842-844.

Koga, T. and N. J. Hoff (1969). The axisymmetric buckling of initially imperfect complete spherical shells. International Journal of Solids and Structures 5(7), 679-97.

Krenzke, M. A. and T. J. Kiernan (1965). Test of stiffened and unstiffened machined spherical shells under external hydrostatic pressure. David Taylor Model Basin, report 1741, S-R0110101.

Morton, J., P. R. Murray and C. Ruiz (1981). On the buckling design of spherical shells. Journal of Pressure Vessel Technology. Transactions of the ASME 103(3), 261-266.

Pan, B. B. and W. C. Cui (2010). An overview of buckling and ultimate strength of spherical pressure hull under external pressure. Marine Structure 23, 227-240.

Papadopoulos, V. and M. Papadrakakis (2005). The effect of material and thickness variability on the buckling load of shells with random initial imperfections. Comput. Methods Appl. Mech. Engrg. 194, 1405-1426.

Papadopoulos, V. and N. Lagaros (2009). Vulnerability-based robust design optimization of imperfect shell structures. Structural Safety 31, 475-482.

Pranesh, S. B., D. Kumar, V. Subramanian, D.Sathianarayanan and G. A. Ramadass (2017). Non-linear buckling analysis of imperfect thin spherical pressure hull for manned submersible. Journal of Ocean Engineering and Science 2(4), 293-300.

Schenk, C. A. and G. I. Schuëller (2003). Buckling analysis of cylindrical shells with random geometric imperfections. International Journal of Non-Linear Mechanics 38, 1119-1132.

Schenk, C. A. and G. I. Schuëller (2007). Buckling analysis of cylindrical shells with cutouts including random boundary and geometric imperfections. Comput. Methods Appl. Mech. Engrg. 196(35-36), 3424-3434.

Teng, J. G. and J. M. Rotter (2004). Buckling of Thin Metal Shells. London and New York: Spon Press.

Yu, C. Y., Z. T. Chen, C. Chen and Y. T. Chen (2017). Influence of initial imperfections on ultimate strength of spherical shells. International Journal of Naval Architecture and Ocean Engineering 9, 473-483.

Zhang, J., M. Zhang, W. Cui, W. Tang, F. Wang and B. Pan (2018). Elastic-plastic buckling of deep sea spherical pressure hulls. Marine Structures 57, 38-51.